J Wood Sci (2005) 51:566–571
DOI 10.1007/s10086-005-0700-4

ORIGINAL ARTICLE

Jørgen Lauritzen Jensen

Quasi-non-linear fracture mechanics analysis of the double cantilever beam specimen

Received: July 26, 2004 / Accepted: January 5, 2005

Abstract A quasi-non-linear fracture mechanics model based on beam on elastic foundation theory is applied for analysis of the double cantilever beam (DCB) specimen for determination of fracture energy of wood. The properties of the elastic foundation are chosen so that the perpendicular-to-grain tensile strength and fracture energy properties of the wood are correctly represented. It is shown that this particular choice of foundation stiffness makes a conventional maximum stress failure criterion lead to the same solution as the fracture mechanics compliance method. Results of linear elastic fracture mechanics are obtained as a special case by assuming an infinitely large value of the perpendicular-to-grain tensile strength. The quasi-non-linear fracture mechanics model is compared with other models and with results of tests conducted to reveal the influence of the geometrical properties of the DCB specimen. In addition, the appropriateness of choice of the foundation stiffness is investigated.

Key words DCB specimen · Fracture energy · Beam on elastic foundation · Foundation stiffness · Quasi-non-linear fracture mechanics

Introduction

Mode I fracture energy of wood may be determined experimentally using, e.g., small tension specimens[1] or a notched specimen in a three-point bending test[2] recording the complete load–deflection relationship. A much easier experimental method, however, is to use a double cantilever beam (DCB) specimen as shown in Fig. 1. The DCB specimen has been adopted in ASTM D3433[3] for determination of the critical energy release rate of bond lines using adherends of steel, but no major testing standard seems yet to have adopted the DCB specimen for determination of the mode I critical energy release rate or the fracture energy of wood.

Using the DCB specimen, however, the critical energy release rate is not determined directly by testing, but is derived from test results through some theoretical models. Thus, the value of the critical energy release rate depends on the assumptions adopted in the theoretical model. A number of theoretical expressions for determination of the critical energy release rate for wooden DCB specimens have previously been presented,[1,4,5] some of which are based on beam on elastic foundation (BEF) theory.

The model presented in this article is likewise based on BEF theory. The main new feature in the model presented here is the definition of the foundation modulus. Previous models have associated the foundation modulus with the elastic strain in the wood, i.e., a function of the perpendicular-to-grain modulus of elasticity (MOE) and the dimension of the wood member in the perpendicular-to-grain direction, whereas the present model associates the foundation modulus with the fracture performance of the wood, i.e., perpendicular-to-grain tensile strength and mode I fracture energy. Furthermore, the present model is based on Timoshenko beam theory, i.e., the shear deformations are taken into account, and a finite length of the initially uncracked part of the specimen is considered.

Theory

A beam on elastic foundation is schematically shown in Fig. 2. The deflections and rotations of the beam axis are denoted $w(x)$ and $\theta(x)$, respectively. Of special interest here is $w_0 = w(0)$ and $\theta_0 = \theta(0)$, of which positive directions are indicated in the figure.

For a Timoshenko beam on elastic foundation,[6] w_0 and θ_0 may be written

$$w_0 = \frac{P}{EI}\frac{c_3 + c_1 a}{c}, \qquad \theta_0 = \frac{P}{EI}\frac{c_1 + c_2 a}{c} \tag{1}$$

J.L. Jensen (✉)
Institute of Wood Technology, Akita Prefectural University,
11-1 Kaieizaka, Noshiro 016-0876, Japan
Tel. +81-185-52-6985; Fax +81-185-52-6976
e-mail: jensen@iwt.akita-pu.ac.jp

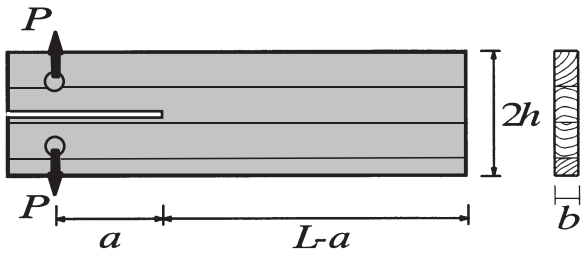

Fig. 1. Geometry of double cantilever beam (DCB) specimen

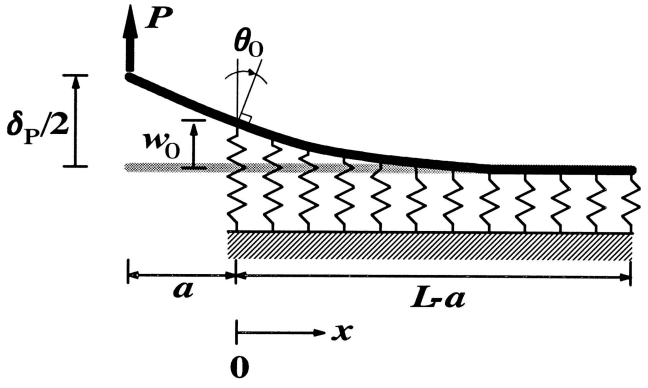

Fig. 2. Symmetrical half of DCB specimen modeled as beam on elastic foundation

where the definitions of c, c_1, c_2, and c_3 are given by Eq. 3, and P is the applied load as shown in Figs. 1 and 2.

In addition, the parameters λ and η are defined as

$$\lambda = \frac{Kb}{EI}, \qquad \eta = \frac{Kb}{GA_s} \tag{2}$$

where b is the width, I is moment of inertia, and A_s is equivalent shear area ($I = bh^3/12$ and $A_s = 5bh/6$ for a rectangular cross section), E is the parallel-to-grain modulus of elasticity, G is the shear modulus, and K is the foundation modulus (unit: N/m^3).

The solution to the governing differential equations is divided into two cases, and the c constants in Eq. 1 are given by

Case I: $\lambda \geq {}^1/_4\eta^2$

$$v^2 = \frac{1}{2}\sqrt{\lambda} + \frac{1}{4}\eta, \qquad u^2 = \frac{1}{2}\sqrt{\lambda} - \frac{1}{4}\eta$$

$$\begin{aligned}
c &= \sqrt{\lambda}\left[u^2\sinh^2 v(L-a) - v^2\sin^2 u(L-a)\right] \\
c_1 &= v^2\sin^2 u(L-a) + u^2\sinh^2 v(L-a) \\
c_2 &= 2vu\left[u\cosh v(L-a)\sinh v(L-a)\right. \\
&\quad \left. + v\cos u(L-a)\sin u(L-a)\right] \\
c_3 &= \frac{2vu}{\sqrt{\lambda}}\left[u\cosh v(L-a)\sinh v(L-a)\right. \\
&\quad \left. - v\cos u(L-s)\sin u(L-a)\right]
\end{aligned} \tag{3a}$$

Case II: $\lambda < {}^1/_4\eta^2$

$$v^2 = \frac{1}{2}\eta + \sqrt{\frac{1}{4}\eta^2 - \lambda}, \qquad u^2 = \frac{1}{2}\eta - \sqrt{\frac{1}{4}\eta^2 - \lambda}$$

$$\begin{aligned}
c &= \eta vu\sinh v(L-a)\sinh u(L-a) \\
&\quad - 2\lambda\left[\cosh v(L-a)\cosh u(L-a) - 1\right] \\
c_1 &= \eta\left[\cosh v(L-a)\cosh u(L-a) - 1\right] \\
&\quad - 2\sqrt{\lambda}\sinh v(L-a)\sinh u(L-a) \\
c_2 &= \left(v^2 - u^2\right)\left[v\sinh v(L-a)\cosh u(L-a)\right. \\
&\quad \left. - u\cosh v(L-a)\sinh u(L-a)\right] \\
c_3 &= \left(\frac{v^2}{u^2} - 1\right)u\cosh v(L-a)\sinh u(L-a) \\
&\quad + \left(\frac{u^2}{v^2} - 1\right)v\cosh u(L-a)\sinh v(L-a)
\end{aligned} \tag{3b}$$

Energy release rate failure criterion

The deflection δ_P at the loading point may be written

$$\delta_P = \delta_{Pc} + \delta_{Pw} + \delta_{P\theta} \tag{4}$$

where δ_{Pc} is the contribution from the cantilever according to ordinary beam theory

$$\delta_{Pc} = 2\left(\frac{a^3}{3EI} + \frac{6a}{5GA}\right)P \tag{5}$$

and $(\delta_{Pw} + \delta_{P\theta})$ is the contribution from the beam on elastic foundation

$$\delta_{Pw} + \delta_{P\theta} = 2\left(w_0 + a\theta_0\right) = \frac{2}{EI}\frac{1}{c}\left(c_3 + 2c_1 a + c_2 a^2\right)P \tag{6}$$

The compliance, C, is given by

$$C = \frac{\delta_P}{P} = \frac{2}{EI}\left(\frac{a^3}{3} + \frac{6}{5}\frac{EI}{GA}a + \frac{1}{c}\left(c_3 + 2c_1 a + c_2 a^2\right)\right) \tag{7}$$

For a linear elastic body loaded by a single load, P, the crack propagation energy release rate, $\mathcal{G}$, is given by[7]

$$\mathcal{G} = \frac{P^2}{2b}\frac{\mathrm{d}C}{\mathrm{d}a} \tag{8}$$

A crack starts propagating when the energy release rate assumes a critical value, $\mathcal{G}_c$, i.e., the failure criterion is

$$\mathcal{G} = \mathcal{G}_c \tag{9}$$

Assuming static or quasi-static conditions and no energy dissipation outside the fracture region, the critical energy release rate is equal to the material property fracture energy, $\mathcal{G}_f$, i.e.,

$$\mathcal{G}_c = \mathcal{G}_f \tag{10}$$

From Eqs. 8–10 it follows

$$P_c = \sqrt{\frac{2b\mathcal{G}_f}{\frac{dC}{da}}} \tag{11}$$

For an infinitely long beam [$(L - a) \to \infty$], Eq. 11 leads to

$$P_{c,inf} = b\sqrt{\frac{1}{12}hE\mathcal{G}_f}\left(\frac{h}{a + \Delta a}\right), \qquad \Delta a = h\sqrt{\frac{1}{10}\frac{E}{G} + \sqrt{\frac{E}{3hK}}} \tag{12}$$

Maximum stress failure criterion

The maximum tensile stress in the foundation occurs at $x = 0$ and is given by

$$\sigma_0 = Kw_0 \tag{13}$$

Failure is here assumed to occur when the maximum tensile stress equals the perpendicular-to-grain tensile strength, i.e.,

$$\sigma_0 = f_t \tag{14}$$

From Eqs. 1, 13, and 14 it follows that

$$P_c = f_t\frac{EI}{K}\frac{c/c_1}{a + c_3/c_1} \tag{15}$$

For an infinitely long beam [$(L - a) \to \infty$], Eq. 15 leads to

$$P_{c,inf} = b\sqrt{\frac{1}{12}hE\frac{f_t^2}{K}}\left(\frac{h}{a + \Delta a}\right), \qquad \Delta a = h\sqrt{\frac{1}{10}\frac{E}{G} + \sqrt{\frac{E}{3hK}}} \tag{16}$$

Foundation properties

The deformation of the foundation may be assumed to be composed of a contribution from a special fracture layer (with no physical thickness) and a contribution from the perpendicular-to-grain elastic strains in the beam as indicated in Fig. 3.

The damage and fracture performance of wood is in general nonlinear, but is in the present analysis represented by a linear response that is equivalent in terms of peak stress, f_t, and fracture energy dissipation, $\mathcal{G}_f$. Because the special fracture layer has no physical perpendicular-to-grain dimension, strain is not defined and the perpendicular-to-grain stress, σ, is used as a constitutive relation as a function of the perpendicular-to-grain deformation, δ_f. The fracture energy of the fracture layer is in general given as

$$\mathcal{G}_f = \int_0^\infty \sigma d\delta_f \tag{17}$$

From Fig. 4, it follows that the stiffness of the linear fracture layer, K_f, is given by

$$K_f = \frac{f_t^2}{2\mathcal{G}_f} \tag{18}$$

The elastic perpendicular-to-grain strain, ε_s, in the beam is given by Hook's law, and the deformation, δ_s, and stiffness, K_s, of the part of the DCB specimen between the two beam axes due to elastic strain is thus given by

$$\delta_s = h\varepsilon_s = \frac{h}{E_y}\sigma \quad \Rightarrow \quad K_s = \frac{E_y}{h} \tag{19}$$

From Fig. 3, it follows for the foundation

$$\delta(x) = 2w(x) = \delta_f(x) + \delta_s(x) = \left(\frac{1}{K_f} + \frac{1}{K_s}\right)\sigma(x) \tag{20}$$

or

$$\delta(x) = Kw(x), \qquad K = \frac{2K_fK_s}{K_f + K_s}, \qquad K_f = \frac{f_t^2}{2\mathcal{G}_f}, \qquad K_s = \frac{E_y}{h} \tag{21}$$

In previous applications of beam on elastic foundation theory to fracture problems,[1,5,8] the special fracture layer as considered in the present article has been omitted, and the foundation deformations have been attributed solely to the elastic perpendicular-to-grain strains, i.e., $K_f \to \infty$ resulting in $K = 2E_y/h$ has been assumed. If disregarding the elastic perpendicular-to-grain strains, i.e., $K_s \to \infty$, then

$$K = 2K_f = \frac{f_t^2}{\mathcal{G}_f} \tag{22}$$

From Eqs. 12 and 16 it follows immediately, that the energy release rate criterion and the maximum stress failure crite-

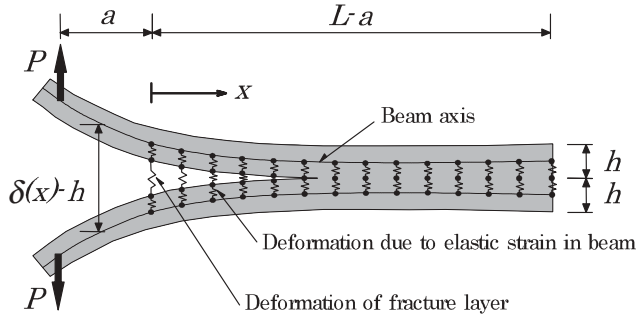

Fig. 3. Foundation model

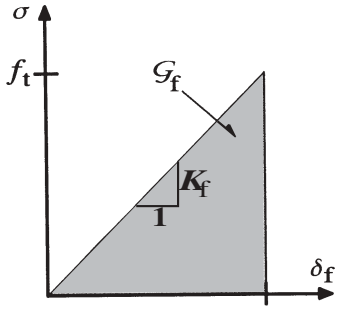

Fig. 4. Constitutive relation of fracture layer

rion lead to the same solution if (and only if) $K = f_t^2/G_f$. This can also be shown to hold true for the general solutions given by Eqs. 11 and 15.

The present strength analysis of mode I failure using beam on elastic foundation theory and introducing a special deformation layer with stiffness as given by Eq. 22 is a complete analogy to the fracture mechanics application of the Volkersen model to strength analysis of mode II failure in lap joints.[9] The analysis has been termed quasi-non-linear fracture mechanics because the material responses are assumed to be linear as in linear elastic fracture mechanics (LEFM). However, at the same time the tensile strength is assigned a finite value, not an infinite value as in LEFM, and a finite, nonzero size of the fracture region is considered, leading to a failure load that is not proportional to the square root of the fracture energy.

Fracture energy

Using the foundation modulus as given by Eq. 22, Eqs. 11 and 15 give the same failure load and the fracture energy may be calculated from

$$\mathcal{G}_f = \frac{P_c^2}{bEI}\left(\frac{a + \Delta a}{\beta}\right)^2 \qquad \beta = \frac{c}{\sqrt{\lambda c_1}}, \qquad \Delta a = \frac{c_3}{c_1} \tag{23}$$

where the c functions are given in Eq. 3, and $I = bh^3/12$.

For an infinitely long specimen $[(L - a) \to \infty]$, Eqs. 12 and 21 lead to

$$\mathcal{G}_f = \frac{P_c^2}{bEI}(a + \Delta a)^2, \qquad \Delta a = h\sqrt{\frac{1}{10}\frac{E}{G} + \varepsilon},$$
$$\varepsilon = \sqrt{\frac{1}{6h}\left(\frac{hE}{E_y} + \frac{2E\mathcal{G}_f}{f_t^2}\right)} \tag{24}$$

Especially

$$\varepsilon \to \begin{cases} \sqrt{\dfrac{E}{6E_y}} & \text{for} \quad f_t \to \infty \left(\text{i.e. } K \to \dfrac{2E_y}{h}\right) \\ \dfrac{1}{f_t}\sqrt{\dfrac{E\mathcal{G}_f}{3h}} & \text{for} \quad E_y \to \infty \left(\text{i.e. } K \to \dfrac{f_t^2}{\mathcal{G}_f}\right) \end{cases} \tag{25}$$

Gustafsson and Larsen[4] presented a solution based on LEFM (but not on beam on elastic foundation theory) and arrived at Eq. 24 with $\varepsilon = 0$. That solution is obtained from Eq. 12 if assuming $K \to \infty$.

If the cantilevers of the DCB specimen are considered to be rigidly clamped at the end of the initial crack tip, the compliance method leads to

$$\mathcal{G}_f = \frac{P_c^2}{bEI}\left(a^2 + \frac{1}{10}\frac{E}{G}h^2\right) \tag{26}$$

ASTM D3433-93[3] gives the following formula for determination of the fracture energy

$$\mathcal{G}_f = \frac{P_c^2}{bEI}\left(a^2 + \frac{1}{3}h^2\right) \tag{27}$$

Equations 23 and 24 do, in general, not provide explicit expressions for calculation of the fracture energy. However, a reasonable initial guess of $\mathcal{G}_f$ used in the right side of Eq. 23 or 24 usually results in convergence of $\mathcal{G}_f$ after just two to three successive calculations. Another disadvantage of using $K = f_t^2/\mathcal{G}_f$ is that it involves the perpendicular-to-grain tensile strength of wood, which is highly volume dependent. A relevant size of a tension test specimen for direct determination of f_t is not obvious.

So-called plate joint test specimens have previously been proposed for deriving relevant fracture properties for use in LEFM models,[4,10] and may in principle also be used for determination of the perpendicular-to-grain tensile strength by means of a quasi-non-linear fracture mechanics model.[11] However, the plate joint specimen is relatively insensitive to variations in f_t in the relevant range, and therefore seems inappropriate. Fortunately, it appears that the DCB specimen is also not sensitive to variations in f_t in the relevant range for sufficiently large a/h ratios. Figure 5 shows the failure load as predicted by Eq. 12 or 16 and Eq. 22 using $b = 20$ mm, $h = 50$ mm, $E = 8340$ MPa, $G = E/18$, and $\mathcal{G}_f = 0.23$ N/mm. It may even be considered to use DCB specimens with large a/h ratios for determination of $\mathcal{G}_f$, and DCB specimens with small a/h ratios for determination of f_t.

Experimental

Tests were conducted on DCB specimens in order to evaluate the difference in fracture energy determined by different theoretical models and to evaluate the influence of initial crack length, a, and the length of initially noncracked length, $L - a$. In addition, tests were conducted to evaluate the influence of elastic perpendicular-to-grain strains.

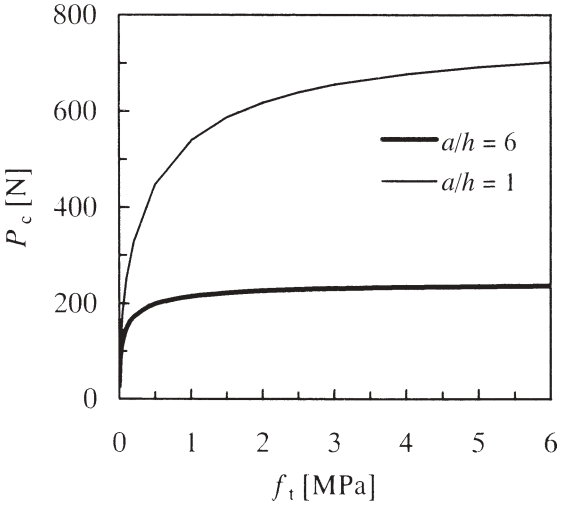

Fig. 5. Influence of f_t on the failure load

Methods and materials

All specimens were made of glulam of Japanese cedar (*Cryptomeria japonica*). The laminae, thickness 30 mm, were all of the same grade and without finger joints. The MOE in the grain direction was determined by measuring the longitudinal vibration frequency of the glulam beams, from which the specimens were cut. All tests were displacement controlled. All DCB specimens were tested so that failure occurred after 2–3 min, the time to failure for the tension specimens was about 30 seconds.

Three test series were conducted on DCB specimens, as shown in Fig. 1. The initial crack was made by drilling a 3-mm hole at the location of the initial crack tip and then cutting a 2-mm-wide slit from the end of the specimen to the hole.

Series 1 was conducted to evaluate the influence of the initial crack length, a. All specimens had the dimensions of $b = 20$ mm, $h = 50$ mm, $L = 600$ mm. Ratios $a/h = 1$, 2, 4, and 6 were tested. Five specimens were tested for each condition. Moisture content (MC) was 11%, the density was 370 kg/m^3 at 11% MC, and the MOE was 8340 MPa. The specimens were not specially selected to avoid defects in the vicinity of the crack tip.

Series 2 was conducted to evaluate the influence of the length of the initially uncracked part, $L - a$. All specimens had the dimensions of $b = 20$ mm, $h = 50$ mm, $a = 100$ mm. The number of specimens were 6, 12, 10, and 12 for the tested ratios $(L - a)/h = 2$, 4, 6, and 12, respectively. The MC was 14%, density was 384 kg/m^3 at 14% MC, and the MOE was 8959 MPa.

Series 3 was conducted to evaluate the influence of beam depth, h. Specimens with the dimensions of $b = 20$ mm, $a = 2h$, and $(L - a) = 4h$ were tested for $h = 20$ mm, 50 mm, and 100 mm. Six specimens were tested for each condition. The MC was 13%, density was 358 kg/m^3 at 13% MC, and the MOE was 7914 MPa. All specimens for this test series were cut from the same glulam beam, and in such a way that the initial cracks were all located in the same lamina. The specimens were carefully selected to avoid defects in the vicinity of the crack tip.

Tension tests were conducted on specimens as shown in Fig. 6. The specimens were cut from the same beam as the DCB specimens of test series 2, and in such a way that failure in the two specimen types occurred in the same lamina. Six specimens were tested.

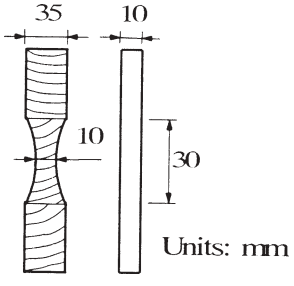

Fig. 6. Test specimen for determination of perpendicular-to-grain tensile strength

Results and discussion

The tension tests gave a value of the perpendicular-to-grain tensile strength, f_t, of 3.9 ± 0.9 MPa (mean value ± standard deviation). Table 1 shows the mean values of the fracture energy as determined by the use of Eqs. 24, 26, and 27 given for test series 1. It may be worthy of notice that the more elaborate a model (i.e., the more contributions are taken into account for calculation of the compliance), the higher values of the fracture energy are obtained. This fact may be a general point of concern. If for instance Eq. 24 is used in a testing standard for determination of the fracture energy, and this value of the fracture energy is used for calculation of the load-carrying capacity using a less elaborate model (say Eq. 27), an unsafe solution is obtained. Using $K = f_t^2/G_f$ will always produce safe values of the fracture energy as compared with K as given by Eq. 21, and in most practical cases will also produce safe values as compared with $K = 2E_y/h$.

Figure 7 shows the failure loads of test series 2. The mean values of the failure loads for $(L - a)/h = 4$, 6, and 12 are not significantly different, while $(L - a)/h = 2$ gives a significantly lower mean failure load. The theoretical failure load as predicted by Eqs. 15 and 22 using $G_f = 0.23$ N/mm (which is the mean value determined from test series 1 for $a/h = 2$, 4, and 6) is also shown for $f_t = 3.9$ MPa as obtained by the tension tests and for a value $f_t = 2.3$ MPa chosen in order

Table 1. Fracture energy determined for test series 1

Equation	a/h			
	1	2	4	6
24	0.26	0.27	0.27	0.24
24 ($f_t \to \infty$)	0.25	0.26	0.26	0.24
24 ($E_y \to \infty$)	0.20	0.22	0.23	0.22
24 ($\varepsilon = 0$)	0.16	0.19	0.21	0.20
26	0.08	0.10	0.13	0.14
27	0.04	0.07	0.12	0.14

Units: N/mm

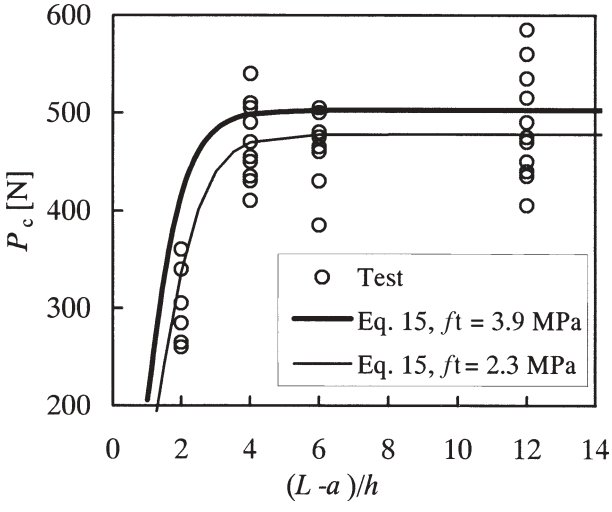

Fig. 7. Failure loads of test series 2

Table 2. Fracture energy of test series 3 using Eq. 24

Specimen	h (mm)	a (mm)	$\mathcal{G}_f$ (N/mm)	
			$E_y \to \infty$	$f_t \to \infty$
1	20	40	0.16	0.18
2	50	100	0.15	0.18
3	100	200	0.18	0.23

Table 3. Calculated and tested failure loads of test series 3

Equation	K	P_{c1} (N)	P_{c3} (N)	P_{c1}/P_{c3}
12	$f_t^2/\mathcal{G}_f$	237	558	0.42
16	$f_t^2/\mathcal{G}_f$	237	558	0.42
12	$2E_y/h$	244	546	0.45
16	$2E_y/h$	402	2010	0.20
Test		248	614	0.40

P_{c1}, failure load of specimen 1 (h = 20 mm); P_{c3}, failure load of specimen 3 (h = 100 mm)

to fit the test results well. The model is seen to be able to predict the influence of the initially uncracked length, $L - a$, in good agreement with the test results.

Table 2 shows the fracture energy determined for series 3 using Eq. 24 with $E_y \to \infty$ (i.e., $K = f_t^2/\mathcal{G}_f$) and $f_t \to \infty$ (i.e., $K = 2E_y/h$). The fracture energy of test series 3 is significantly lower than the values determined for test series 1 and 2. This is due to the fact that all specimens of test series 3 were taken from the same beam and carefully selected so as to avoid any defects, which have a reinforcing effect, in the vicinity of the crack tip.

Table 3 shows the failure loads, P_{c1} and P_{c3}, of test specimens 1 and 3 (see Table 2), respectively, as obtained by testing and as predicted by Eqs. 12 and 16 using $K = f_t^2/\mathcal{G}_f$ (i.e., $E_y \to \infty$) and $K = 2E_y/h$ (i.e., $f_t \to \infty$). Specimen 2 (h = 50 mm, a = 100 mm) was used for determination of the fracture energy as given in Table 2. Because a constant value $a/h = 2$ was used for all specimens, Eq. 12 with $K = 2E_y/h$ leads to $P_{c1}/P_{c3} = (h_1/h_3)^{1/2}$ and Eq. 16 with $K = 2E_y/h$ leads to $P_{c1}/P_{c3} = h_1/h_3$, which are independent of f_t and $\mathcal{G}_f$.

Table 3 also shows that the maximum stress failure criterion (Eq. 16) is in severe disagreement with test results if using $K = 2E_y/h$, while $K = f_t^2/\mathcal{G}_f$ leads to agreement. However, the two different foundation moduli both result in good agreement between theory and tests if used with the compliance approach (Eq. 12).

Conclusions

A model for analysis of the double cantilever beam specimen for determination of the fracture energy of wood was presented. The model is based on linear elastic Timoshenko beam on elastic foundation theory, which includes shear deformations and takes into account the finite length of the initially uncracked part of the DCB specimen. The analysis, which may be characterized as a quasi-non-linear fracture mechanics analysis, includes a fracture mechanics approach based on the compliance method and a conventional stress approach. It was shown that a particular choice of the properties of the elastic foundation, which ensures that the perpendicular-to-grain tensile strength and fracture energy properties of the wood are correctly represented, makes the two approaches lead to the same solution. Previous models using beam on elastic foundation theory seem all to have related the stiffness of the foundation solely to the elastic perpendicular-to-grain strains, which leads to the fact that the compliance method and stress approaches, in general, lead to significantly different results.

Tests were conducted to evaluate the influence of the length of the initial crack and of the length of the initially uncracked (beam on elastic foundation) part of the DCB specimen. Theoretically predicted results were found to be in very good agreement with test results.

Tests were also conducted on DCB specimens with various depths in order to evaluate the appropriate choice of foundation properties. The tests revealed that relating the foundation stiffness to the elastic perpendicular-to-grain strains leads to good agreement between theory and tests if used with the compliance method approach, but to very poor results if used with the stress approach. The new estimation of the foundation stiffness as presented in this article unifies the compliance method and stress approaches and leads to good agreement with test results.

References

1. Wernersson H (1994) Fracture characterization of wood adhesive joints. Report TVSM-1006, Lund University, Lund Institute of Technology, Division of Structural Mechanics, Sweden
2. Gustafsson PJ (2003) Fracture perpendicular to grain – structural applications. In: Thelandersson S Larsen HJ (eds) Timber engineering. Wiley, Chichester, pp 103–130
3. American Society for Testing and Materials (1995) ASTM D 3433 – 93, Standard test method for fracture strength in cleavage of adhesives in bonded metal joints. In: Annual Book of ASTM Standards, ASTM, Philadelphia, Vol 15.06, pp 218–224
4. Gustafsson PJ, Larsen HJ (2001) Dowel joints loaded perpendicular to grain. In: Aicher S, Reinhardt HW (eds) Joints in timber structures. Proceedings of the International RILEM Symposium, Stuttgart, Germany, pp 577–586
5. Komatsu K, Sasaki H, Maku T (1976) Strain energy release rate of double cantilever beam specimen with finite thickness of adhesive layer. Wood Res 59:80–92
6. Pilkey WD (1994) Formulas for stress, strain, and structural matrices. Wiley, New York, pp 534–545
7. Hellan K (1984) Introduction to fracture mechanics. McGraw-Hill, New York, pp 49–72
8. Jorissen AJM (1998) Double shear timber connections with dowel type fasteners. Delft University Press, Delft, The Netherlands
9. Gustafsson PJ (1987) Analysis of generalized Volkersen-joints in terms of non-linear fracture mechanics. In: Verchery G, Cardon AH (eds) Mechanical behaviour of adhesive joints. Pluralis, Paris, pp 323–338
10. Yasumura M (2002) Determination of fracture parameter for dowel-type joints loaded perpendicular to wooden grain and its application. In: Proceedings of the International Council for Research and Innovation in Building and Construction, CIB-W18 Meeting Thirty-Five, Kyoto, Japan, paper No. 35-7-9
11. Jensen JL (2005) Quasi-non-linear fracture mechanics analysis of the splitting failure of single dowel joints loaded perpendicular to grain. J Wood Sci 51:559–565